SCIENCE CHINA
Technological Sciences

• Article •

April 2017 Vol.60 No.4: 624–637
doi: 10.1007/s11431-016-0460-2

Finite element analysis for inclined wellbore stability of transversely iso-tropic rock with HMCD coupling based on weak plane strength criterion

WANG YongLiang[1,2*], ZHUANG Zhuo[1], LIU ZhanLi[1], YANG HengLin[3] & LI ChenFeng[2]

[1]*Applied Mechanics Laboratory, School of Aerospace Engineering, Tsinghua University, Beijing 100084, China;*
[2]*Zienkiewicz Centre for Computational Engineering & Energy Safety Research Institute, College of Engineering, Swansea University, Swansea SA2 8PP, UK;*
[3]*Drilling Research Institute, China National Petroleum Corporation, Beijing 100195, China*

Received June 12, 2016; accepted October 7, 2016; published online December 14, 2016

The finite element analysis (FEA) technology by hydraulic-mechanical-chemical-damage (HMCD) coupling is proposed in this paper for inclined wellbore stability analysis of water-sensitive and laminated rock, developed basing on the recently established FEA technology for transversely isotropic rock with hydraulic-mechanical-damage (HMD) coupling. The chemical activity of the drilling fluid is considered as phenomenological hydration behavior, the moisture content and parameters of rock considering hydration could be determined with time. The finite element (FE) solutions of numerical wellbore model considering the chemical activity of drilling fluid, damage tensor calculation and weak plane strength criterion for transversely isotropic rock are developed for researching the wellbore failure characteristics and computing the time-dependent collapse and fracture pressure of laminated rock as shale reservoirs. A three-dimensional FE model and elastic solid deformation and seepage flow coupled equations are developed, and the damage tensor calculation technology for transversely isotropic rock are realized by introducing effect of the hydration and the stress state under the current load. The proposed method utilizing weak plane strength criterion fully reflects the strength parameters in rock matrix and weak plane. To the end, an effective and reliable numerically three-step FEA strategy is well established for wellbore stability analysis. Numerical examples are given to show that the proposed method can establish efficient and applicable FE model and be suitable for analyzing the time-dependent solutions of pore pressure and stresses, and the evolution region considering the hydration surrounding wellbore, furthermore to compute the collapse cycling time and the safe mud weight for collapse and fracture pressure of transversely isotropic rock.

finite element analysis, wellbore stability, transversely isotropic rock, hydraulic-mechanical-chemical-damage coupling, weak plane strength criterion

Citation: Wang Y L, Zhuang Z, Liu Z L, et al. Finite element analysis for inclined wellbore stability of transversely iso-tropic rock with HMCD coupling based on weak plane strength criterion. Sci China Tech Sci, 2017, 60: 624–637, doi: 10.1007/s11431-016-0460-2

1 Introduction

The wellbore instability problems appeared in shale gas exploitation due to the anisotropic mechanical behaviors of unconventional shale [1]. Shale exhibits typical water-sensitive and laminated characteristics. By experiment researches, shale is composed by fabric-related and plate-like minerals [2,3], in which material and strength parameters possess apparent heterogeneity and typical transversely iso-

*Corresponding author (email: wangyongliang@tsinghua.edu.cn)

tropic behavior [4]. Chemically active effect of drilling fluid is considered as the important influencing factor for wellbore stability of mud shale when drilling [5]. The stability problem of a wellbore drilled into a thinly laminated anisotropic rock formation in this paper is shown in Figure 1, which is assumed in transversely isotropic formation coordinate system (TCS) x_t–y_t–z_t; the plane parallel and direction vertical to bedding are frequently replaced below by the terminologies as isotropic plan and transverse direction respectively. Drilling a borehole with a given mud pressure P into formation, which is fully saturated with a pore fluid and subjected to the preexisting *in-situ* stresses (S_H is maximum horizontal principal stress, S_h is minimum horizontal principal stress, S_v is vertical stress) initially in static equilibrium, disturbs the state of stress in the vicinity of borehole. The finite element analysis (FEA) technology presented in this paper takes water-sensitive and laminated rock as the research object, a typical porous medium with transversely isotropic property and strength, dispersedly distributed damage region under applied mud pressure and *in-situ* stresses, to obtain the collapse cycling time, collapse and fracture pressure as safe mud weight.

Shale has the characteristic of low porosity and permeability as unconventional rock, particularly the key technology of horizontal well drilling could create damage and crack propagation around the wellbore, to change the porosity and permeability [6]. The effective stress of porous medium will change with the fluid flow, pressure diffusion in pores and solid deformation correspondingly, in other words, hydraulic-mechanical (HM) coupling makes the response of the rock reflect complex time-dependent effect obviously. For some conventional and simple problems, such as possessing regular solving domain with homogeneous material property, analytical method via the poroelastic theory has been proposed to solve a number of multi-fields coupling, wellbore stability and fracture problems [7,8], and a related method for an inclined borehole in a special transversely isotropic formation have been developed [9,10]. Utilizing the poroelastic analytical solutions and introducing the isotropic rock strength criterion, a weak plane model for wellbore stability of anisotropic formations had been developed [11]. Rock is a typically heterogeneous, brittle medium with complex damage and breakage occurring under external

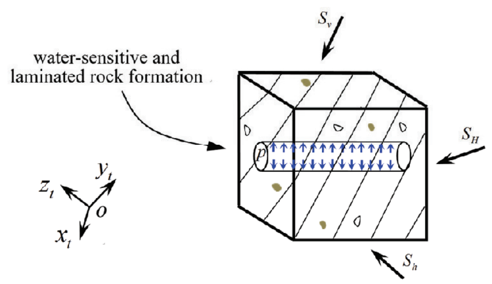

Figure 1 (Color online) Wellbore in water-sensitive and laminated rock formation subjected to *in-situ* stresses.

load [12,13], however, the analytical method unfortunately does not consider heterogeneity, plastic deformation and damage evolution and hence cannot serve as a practical and general method. Therefore, some reseachers were motivated to probe into the numerical area of anisotropic rock fracture, damage analysis and wellbore stability problems. The authors of this paper have made a series of achievements on the basic theory and algorithm of extended finite element method (XFEM) as discrete fracture network model for arbitrary crack growth [14,15]. On the other hand, some researchers proposed the continuous model basing on the damage mechanics to analyze the failure process, compared to discrete fracture network model, which more easily handles the multi-fields coupling and complex medium containing pores and cracks problems to be consistent with the material behavior [16]. Inspired from which, some numerical methods and simulation technologies based on damage analysis are proposed [17,18]. The damage variable discribed the compressive and tensile behavior of rock was developed by mesoscopic damage mechanics in ref. [15]. A novel and simple FEA technology of seepage in rock have been presented yet by authors of this paper with the further development of the continuous model and continuum damage variable [19,20]. The continuum damage variable was developed effectively into a damage tensor introduced the stresses state under the current load and anisotropic strength to consider the bearing capacity; utilizing the damage tensor, this method developed finite element (FE) algorithm to obtain the stress solutions with damage, and apply to the wellbore stability analysis of transversely isotropic rock with hydraulic-mechanical-damage (HMD) coupling [21]. In resent research work, the authors have developed the FEA technology of transversely isotropic rock with hydraulic-mechanical-chemical-damage (HMCD) coupling for simulating the behavor of anisotropic damage evolution [22].

Many researchers dedicated to the anisotropic strength criteria [23,24]. Hill [25] proposed a general criterion expressed as a quadratic function for anisotropic materials, which was not directly applicable to geological materials because the strength behavior of most geological materials is dependent on the hydrostatic stress. Pariseau [26] extended Hill criterion to account for the effect of the hydrostatic stresses. For wellbore stability, weak plane strength criterion [27,28] was considered as a simple, practical and effective criterion. Wellbore stability problems of laminated rock were analyzed using FEM based on the weak plane strength criterion to analyze the failure in rock matrix and weak plane, which was introduced in this paper to check the failure or not.

The FEA technology with HMCD coupling of rock is proposed for water-sensitive and laminated in this paper. In the analysis strategy, a numerical three-dimensional (3D) FE model with *in-situ* stress boundary conditions (BCs) for declined borehole with different inclination and azimuth angle was developed, and FE solutions are obtained using Biot constitutive theory [29,30] and considering hydration effect. Then the effective stress with damage was utilized to obtain both of the collapse pressure (lower mud weight) and fracture pressure (upper mud weight) based on weak plane strength criterion. This yields a FEA technology that is able to establish transversely isotropic rock model and analyze wellbore stability in petroleum engineering applications. Some numerical examples including the below examples have shown that the proposed FEA technology is effective and feasible for inclined wellbore stability of water-sensitive and laminated rock.

2 Transversely isotropy and hydration characterization

2.1 Constitutive equation

The rock reservoir has the typical nonlinear characteristics plastic deformation and damage evolution; however, the nonlinear model will increase the difficulty and calculation cost for analysis, so the linear elastic models could be used in most of the problems. The proposed method in this paper takes the hypothesis of linear elasticity and small deformation, and introduces the damage analysis in the study to describe the nonlinear behavior below. In another hand, the Biot constitutive relation is a well-established constitutive relation for elastic pore medium [31], utilizing which in the proposed method will derivate a coupled HM model. The anisotropic Biot constitutive equation [32] can be expressed as:

$$\bar{\boldsymbol{\sigma}}^{\mathrm{e}} = \boldsymbol{\sigma} - \boldsymbol{\alpha}p = \boldsymbol{C}\bar{\boldsymbol{\varepsilon}} - \boldsymbol{\alpha}p, \tag{1}$$

where $\bar{\boldsymbol{\sigma}}^{\mathrm{e}} = \boldsymbol{\sigma}^{\mathrm{e}} + \Delta\boldsymbol{\sigma}^{\mathrm{e}}$ is the effective stress vector, $\bar{\boldsymbol{\varepsilon}} = \boldsymbol{\varepsilon} + \Delta\boldsymbol{\varepsilon}$ is the strain vector, $\boldsymbol{\sigma}^{\mathrm{e}}$ and ε are effective stress vector $\{\sigma^{\mathrm{e}}_{x_t} \quad \sigma^{\mathrm{e}}_{y_t} \quad \sigma^{\mathrm{e}}_{z_t} \quad \tau^{\mathrm{e}}_{x_t y_t} \quad \tau^{\mathrm{e}}_{y_t z_t} \quad \tau^{\mathrm{e}}_{x_t z_t}\}^{\mathrm{T}}$ and strain vector $\{\varepsilon_{x_t} \quad \varepsilon_{y_t} \quad \varepsilon_{z_t} \quad \gamma_{x_t y_t} \quad \gamma_{y_t z_t} \quad \gamma_{x_t z_t}\}^{\mathrm{T}}$ respectively without considering hydration characterization, $\Delta\boldsymbol{\sigma}^{\mathrm{e}}$ and $\Delta\boldsymbol{\varepsilon}$ are effective stress and strain vector respectively introduced by hydration, the compressive stress and strain are positive throughout in this paper and vice versa; $\boldsymbol{\alpha}$ is Biot coefficient vector as $\{\alpha_x \quad \alpha_y \quad \alpha_z \quad 0 \quad 0 \quad 0\}^{\mathrm{T}}$, in transversely isotropic case, α_x and α_y are equal parameters in isotropic plane expressed as α_h and α_z is parameter in transverse direction expressed as α_v in below content; p is the pore pressure; $\boldsymbol{C}$ is the stiffness matrix. For general anisotropy, the constitutive relation contains twenty-eight independent material coefficients. For materials with three mutually orthogonal planes of elastic symmetry, known as orthotropic, there exist thirteen independent material coefficients; furthermore, stiffness matrix $\boldsymbol{C}$ of transversely isotropic case could be simplified as:

$$\boldsymbol{C} = \begin{bmatrix} M_{11} & M_{12} & M_{13} & 0 & 0 & 0 \\ & M_{11} & M_{13} & 0 & 0 & 0 \\ & & M_{33} & 0 & 0 & 0 \\ & & & M_{44} & 0 & 0 \\ & sym. & & & M_{55} & 0 \\ & & & & & M_{55} \end{bmatrix},$$

where drained elastic modulus can be expressed in terms of engineering constants as:

$$M_{11} = \frac{E_h(E_v - E_h v_v^2)}{(1+v_h)(E_v - E_v v_h - 2E_h v_v^2)},$$
$$M_{12} = \frac{E_h(E_v v_h - E_h v_v^2)}{(1+v_h)(E_v - E_v v_h - 2E_h v_v^2)},$$
$$M_{13} = \frac{E_h E_v v_v}{E_v - E_v v_h - 2E_h v_v^2},$$
$$M_{33} = \frac{E_v^2(1-v_h)}{E_v - E_v v_h - 2E_h v_v^2},$$
$$M_{44} = \frac{E_h}{2(1+v_h)},$$
$$M_{55} = G_v,$$

where E_h and v_h are drained Young's modulus and Poisson's ratio in the isotropic plane, E_v and $\boldsymbol{v}_v$ are similar quantities related to the direction of the axis of symmetry (transverse direction) and G_v is the shear modulus related to the direction of the axis of symmetry. For the convenience of introduce below, the elastic and permeability matrixes could be expressed as:

$$\boldsymbol{e} = \begin{bmatrix} E_{x_t} & G_{x_t y_t} & G_{x_t z_t} \\ & E_{y_t} & G_{y_t z_t} \\ sym. & & E_{z_t} \end{bmatrix}, \quad \boldsymbol{k}_t = \begin{bmatrix} k_{x_t} & k_{x_t y_t} & k_{x_t z_t} \\ & k_{y_t} & k_{y_t z_t} \\ sym. & & k_{z_t} \end{bmatrix},$$

where E_{x_t} and E_{y_t} have the equally initial value E_h; E_{z_t} has the initial value E_v; $G_{x_t y_t}$ has the initial value $G_h = E_h / 2(1+v_h)$, $G_{x_t z_t}$ and $G_{y_t z_t}$ have the initial permeability G_v; k_{x_t} and k_{y_t} have the equally initial permeability k_h in isotropic plane; k_{z_t} has the initial permeability k_v in transverse direction; as the non-diagonal parameters, $k_{x_t y_t}$ and $k_{x_t z_t}$ have the initial permeability k_h, $k_{y_t z_t}$ has the initial permeability k_v.

2.2 Hydration effect

Considering the chemically active effect of rock, some hydration analysis has been carried out for isotropic rock media. The chemical activity of the drilling fluid is considered as phenomenological hydration behavior, which will be introduced in this paper. According to the conservation of fluid mass, the water absorption diffusion equation can be established, and with the boundary conditions, the moisture content and the relationship with other physical parameters at any position and time in rock could be obtained [33,34]. The proposed method in this paper will extend the hydration analysis to the transversely isotropic media form isotropic case, furthermore, the moisture content in isotropic plane and transverse direction could be expressed as:

$$w_k(r,\bar{t}) = w_\infty + (w_{d/2} - w_\infty)\mathrm{erfc}(r/2\sqrt{c_k \bar{t}}), \tag{2}$$

where $w_k(r,\bar{t})$ is moisture content, r is the absolute radial distance form wellbore wall, $\bar{t}$ is the time of water absorption diffusion; $w_{d/2}$ and w_∞ are initial moisture content at wellbore wall and infinity respectively, c_k is adsorption diffusion constant (c_h and c_v for isotropic plane and transversely isotropic respectively); $\mathrm{erfc}(r/2\sqrt{c_k \bar{t}})$ is error compensation function.

On the current moisture content, the hydration expansion strain, elastic and strength parameters with moisture content of isotropic rock media could be established, in which using experimental data to form empirical formulas is effective and practical method in the present researches [30]. The proposed method will apply this technology to the transversely isotropic media, the hydration expansion strain, elastic, Poisson's radio and strength parameters could be expressed as:

$$\Delta\varepsilon_{ij}(r,\bar{t}) = \delta_{ij}[c_{\varepsilon 1} w_k(r,\bar{t}) + c_{\varepsilon 2} w_k^2(r,\bar{t})], \tag{3a}$$

$$e_{ij}(r,\bar{t}) = e_{ij0}\exp\{-c_e[w_k(r,\bar{t}) - w_\infty]^{0.5}\}, \tag{3b}$$

$$\nu_i(r,\bar{t}) = \nu_{i0} + c_\nu w_k(r,\bar{t}), \tag{3c}$$

$$\eta_k(r,\bar{t}) = \eta_{k0} - c_\eta[w_k(r,\bar{t}) - w_\infty], \tag{3d}$$

where $\Delta\varepsilon_{ij}(r,\bar{t})$ is coefficient in hydration expansion strain matrix $\Delta\boldsymbol{\varepsilon}$, $c_{\varepsilon 1}$ and $c_{\varepsilon 2}$ are hydration strain constants, δ_{ij} denotes the Kronecker delt function; e_{ij} is coefficient in elastic matrix $\boldsymbol{e}$, e_{ij0} is initial value, c_e is hydration elastic coefficient; $\nu_i(r,\bar{t})$ is hydration Poisson's radio, ν_{i0} is initial value, c_ν is hydration constant for Poisson's radio; $\eta_k(r,\bar{t})$ is hydration strength, η_{k0} is initial value, c_η is hydration strength constant. The above i and j take 1, 2 and 3, each hydration constant could be determined according to experiments. In order to investigate the chemical characteristic for moisture content $w_k(r,\bar{t})$, Young's modulus $e_{ij}(r,\bar{t})$ and strength $\eta_k(r,\bar{t})$ with time $\bar{t}$, here the dimensionless values in eq. (3) adapting $c_k = c_e = c_\eta = w_\infty = e_{ij0} = \eta_{k0} = 1$ and $w_{d/2} = 2$, the hydration function curves could be obtained as shown in Figure 2. It can be saw that the moisture content $w_k(r,\bar{t})$ is becoming bigger, elastic modulus $e_{ij}(r,\bar{t})$ and strength parameter $\eta_k(r,\bar{t})$ are becoming smaller as time increasing. At the short hydration time $\bar{t} = 0.1$, the variables near the wellbore wall significant change obviously, and the surrounding rock appear change as a result of long-term effect. So the chemically active effect of water-sensitive rock need to be considered, and the time-dependent variables should be solved effectively and reliably.

3 FEA strategy

The FEA technology in this paper achieves the results for wellbore stability analysis of transversely isotropic rock with HMCD coupling by implementing the three-step FEA strategy as below, and the corresponding algorithm is illustrated in Figure 3.

3.1 FE solution

For the wellbore stability problems of laminated rock, the numerical 3D FE model will be established with *in-situ* stress boundary conditions (BCs) for declined borehole with different inclination and azimuth angle, in which model the rock media consider the hydration effect. Under the current pressure load P_n of mud on borehole, the effective stress $\boldsymbol{\sigma}_t^{\mathrm{e}}$ and permeability $\boldsymbol{k}_t$ could be calculated to obtain solutions at time $\bar{t}$ by the standard FEA technology, as described in Section 4.

3.2 Damage tensor calculation

The aforementioned effective stress $\boldsymbol{\sigma}_t^{\mathrm{e}}$ and the compressive or tensile strength are used to calculate the damage tensor $\boldsymbol{D}_t$, and furthermore the stress $\tilde{\boldsymbol{\sigma}}_t$ and permeability $\tilde{\boldsymbol{\kappa}}_t$ with damage could be calculated respectively, by which the damage state of the rock under the current hydration and load could be described in Section 5.

3.3 Wellbore stability analysis

Utilizing the weak pane strength criterion, the stress $\tilde{\boldsymbol{\sigma}}_t$ with damage will be used to check if the compressive or tensile situation happens in the weak plane and rock matrix of laminated rock as described in Section 6. The pressure

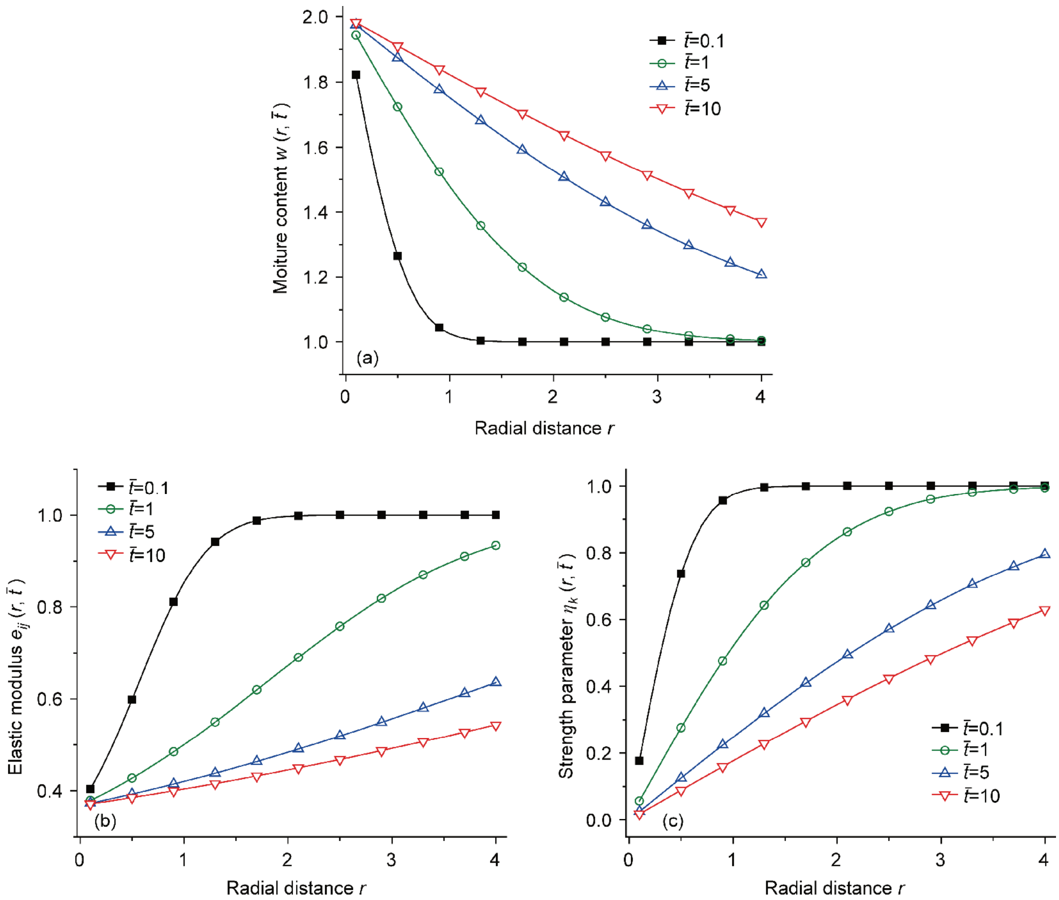

Figure 2 (Color online) Hydration function curves. (a) Moisture content; (b) elastic modulus; (c) strength parameter.

load P_n of mud on borehole will increase a load step ΔP and return to the first step (i.e. FE solution) until both of the collapse pressure (lower mud weight) load interval (P_{cl}, P_{cu}) and fracture pressure (upper mud weight) load interval (P_{fl}, P_{fu}) at time $\bar{t}$ are all achieved.

Because the load intervals (P_l, P_u) for collapse pressure as (P_{cl}, P_{cu}) or fracture pressure as (P_{fl}, P_{fu}) could be too big to obtain the reliable results, the dichotomy method was adapted for selecting the intermediate load $P_a = (P_l + P_u)/2$ to update the upper or lower bound to narrow the intervals, until difference between the upper bound and lower bound is less than the user-preset error tolerance *Tol*, i.e. $P_u - P_l \leqslant Tol$.

The aforementioned three steps constitute a round of FE solving, damage tensor calculation and wellbore stability analysis, by which the instability mode, collapse and fracture pressure of transversely isotropic rock could be obtained to exhibit that there would be obviously different characteristics with isotropic case. The numerical examples below show the proposed FEA strategy is effective, reliable and effective.

4 FE solution

4.1 FE formulation

Utilizing the aforementioned Biot constitutive equation and the hydration analysis technology, the solid and seepage control equations can be discrete utilizing FEM as:

$$\boldsymbol{Ku} = \boldsymbol{P}, \tag{4a}$$

$$(\boldsymbol{H}\Delta\bar{t} + \boldsymbol{S})\boldsymbol{p}_{\bar{t}_{i-1}+\Delta\bar{t}} = \boldsymbol{S}\boldsymbol{p}_{\bar{t}_{i-1}} + \boldsymbol{F}, \tag{4b}$$

where $\boldsymbol{K}$ is the time-dependent stiffness matrix for hydration effect; $\boldsymbol{u}$ is the displacement vector on the FE nodes and $\boldsymbol{P}$ is the load vector; $\boldsymbol{H}$ is conduction matrix; $\boldsymbol{S}$ is memory matrix; $\boldsymbol{F}$ is the fluid convergence vector; $\boldsymbol{p}$ is the pore pressure; here $\bar{t}$ and expressed as superscript is time, $\Delta\bar{t}$ is the time step, $\boldsymbol{p}_{\bar{t}_{i-1}}$ is the pore pressure at $\bar{t}_{i-1}$, $\boldsymbol{p}_{\bar{t}_{i-1}+\Delta\bar{t}}$ is the pore pressure at $\bar{t}_{i-1}+\Delta\bar{t}$. The load $\boldsymbol{P}$ in eq. (4a) consider the pore pressure $\boldsymbol{p}$ as coupling relationship, which pore pressure $\boldsymbol{p}$ is iterative FE solution in eq. (4b). In the proposed method, the transient FE solver of COMSOL Multiphics [35] is taken to obtain the solutions at time $\bar{t}$.

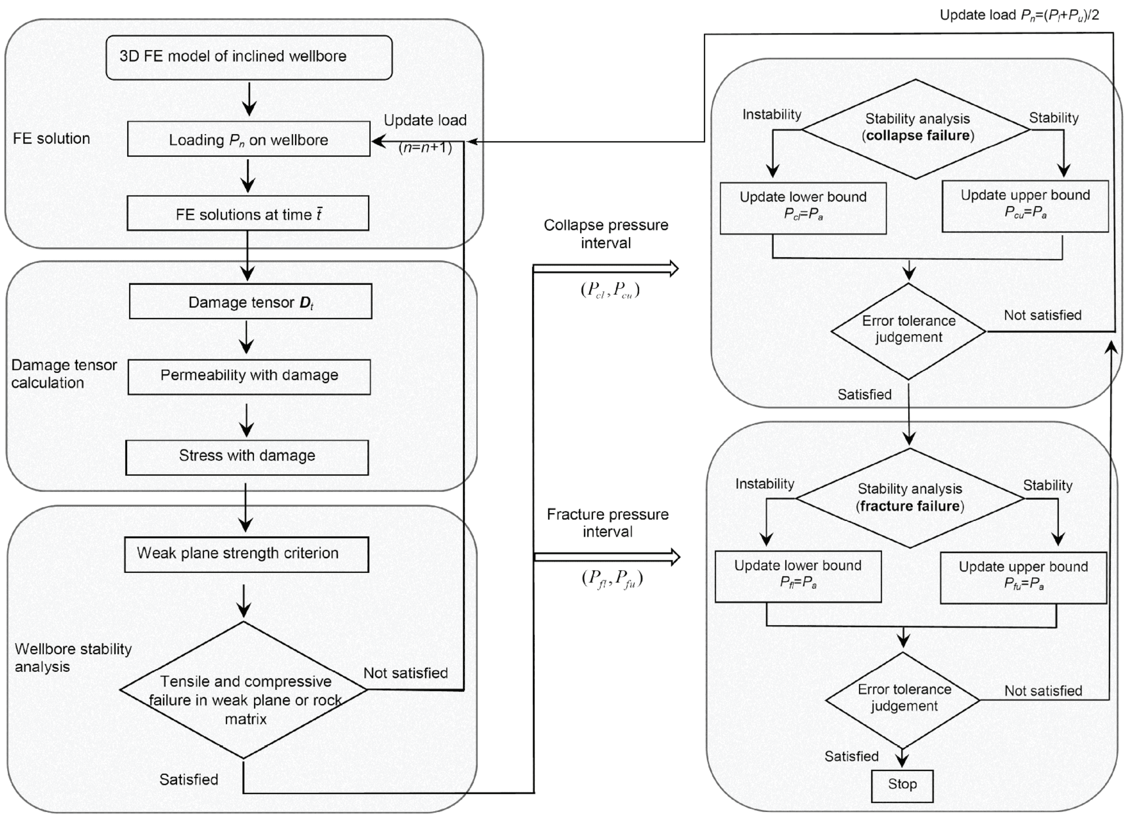

Figure 3 FEA algorithm flowchart of wellbore stability analysis for collapse and fracture pressure computation at time $\bar{t}$.

4.2 FE model for wellbore stability analysis

The inclined wellbore stability model involves multiple stress transformations between the different reference coordinate systems, further four reference coordinated systems are defined as described in the Supporting Information online: global coordinate system (GCS), *in-situ* stress coordinate system (ICS), borehole coordinate system (BCS), and transversely isotropic formation coordinate system (TCS, as mentioned in Figure 1). Each of these and their mutual relationships are shown in Figure S1 (Supporting Information online). Based on the coordinate systems and their relationships defined, the rotation matrices are obtained which are needed to transform stress components from one reference coordinate system to the other [29].

In order to deal with all the *in-situ* stress boundary conditions (BCs) flexibly, the 3D FE model is established in BCS as shown in Figure 4. With the development of the hydration, the drilling fluid expands gradually around the borehole. To reduce the stress concentration effect of *in-situ* stress application, each side length a of the 3D FE model should be at least ten times bigger than the diameter d of the wellbore. According to the established FE model, the stress state of plane at the middle section of the wellbore as Figure 4 is consistent with the practical *in-situ* stress, which technology is suitable by verification of numerical examples containing the examples below, so taking this stress on the plane as the stress state with current well deviation angle and azimuth is appropriate.

In aforementioned 3D FE model, the different types of stress concentration around wellbore will appear in different *in-situ* stress BCs and pressure in borehole, so the mesh at near-field of wellbore should be denser than far-filed to obtain more accurate solutions. On the other hand, too dense mesh would cause overmuch solving time, on the contrary, sometimes denser mesh cannot get more accurate solutions. The meshing method adapted here is adaptive mesh refinement method, by which the user gives an initial coarse FE mesh and specified error tolerance *tol*, and then the computed results on the final adaptive FE mesh will satisfy error tolerance *tol*. This adaptive method has some advantages compared with the traditional FEM, which possess high precision and high efficiency, and suit for different *in-situ* stress BCs and loading conditions. Figure 5 is an adaptive mesh for FE model of inclined wellbore by the proposed method, initial coarse FE mesh is given, and final adaptive FE mesh was obtained as *tol*=5% for controlling the stress solution. From Figure 5, it can be seen that the mesh is become denser automatically in final adaptive mesh than the initial coarse FE mesh, around the wellbore, optimally distributed elements are adopted to handle the problem of stress concentration.

In order to characterize the heterogeneity of rock, in the

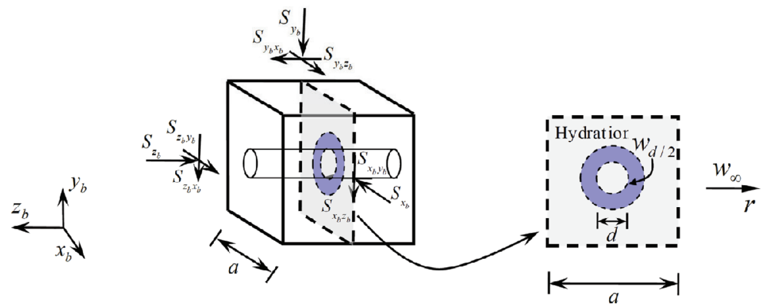

Figure 4 (Color online) FE model and stability analysis plane of inclined wellbore with hydration effect.

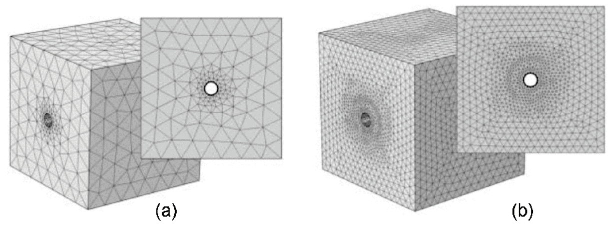

Figure 5 Mesh refinement for FE model of inclined wellbore. (a) Initial coarse FE mesh; (b) final adaptive FE mesh (*tol*=5%).

preliminary study of the authors, the model is discrete as many elements by FEM, and the mechanical properties of each node on FE mesh is assumed to conform to a given Weibull distribution as defined in the following probability density function [17].

$$f(x,\eta,m)=\begin{cases}\dfrac{m}{\eta}\left(\dfrac{x}{\eta}\right)^{m-1}\exp\left[-\left(\dfrac{x}{\eta}\right)^{m}\right], & x\geqslant 0,\\ 0, & x<0,\end{cases} \quad (5)$$

where x is variable representing the mechanical parameter (such as material modulus or strength), η is scale parameter representing the average range of x, m is shape parameter characterizing the homogeneity degree of x. The material property (i.e. Young's modulus E_h and E_v, shear modulus G_v, permeability k_h and k_v) or strength property could describe the heterogeneity of rock, which obey the aforementioned Weibull distribution. The heterogeneity simulation method will be introduced directly in the proposed method of this paper.

5 Damage tensor calculation

In practical engineering, rock is typical brittle material in which damage will occur in some micro-units and expand continuously under load, by continuum damage mechanics, the damage variable describing process of microscopic damage to macroscopic crack deduces the constitutive equation with damage coupling [36]. For wellbore stability problem, ignoring the effect of damage, load-bearing capacity must be overestimated to emerge the instability phenomenon, so damage analysis has been introduced to describe the failure behavior of rock. One of the key techniques incorporated into this procedure is the technology transfer of damage analysis for rock from recently developed transversely isotropic continuum damage with HMD coupling to HMCD coupling by introducing the hydration effect.

5.1 Damage tensor

The chemically active effect for elastic modulus reduction could be saw as damage evolution, combining the hydration of elastic modulus eq. (3b) and the damage definition of elastic modulus reduction [14], the transversely isotropic damage tensor of hydration could be expressed as:

$$\boldsymbol{D}_c=\begin{bmatrix}D_{cx_t} & D_{cx_ty_t} & D_{cx_tz_t}\\ & D_{cy_t} & D_{cy_tz_t}\\ sym. & & D_{cz_t}\end{bmatrix}=\begin{bmatrix}h(w_h) & h(w_h) & h(w_v)\\ & h(w_h) & h(w_v)\\ sym. & & h(w_v)\end{bmatrix}, \quad (6)$$

where $\boldsymbol{D}_c$ is damage tensor of hydration with symmetric property, $h(w_k)=1-\exp\{-c_e[w_k(r,\bar{t})-w_\infty]^{0.5}\}$ is the hydration damage function.

For the transversely isotropic medium, the damage may occur in each principle direction depending on the stress state under the current loud and the anisotropic strength property. In this paper, the uniaxial tensile, compressive and shear strength are introduced and damage variable developed into the damage tensor as [19]:

$$\boldsymbol{D}_m=\begin{bmatrix}D_{mx_t} & D_{mx_ty_t} & D_{mx_tz_t}\\ & D_{my_t} & D_{my_tz_t}\\ sym. & & D_{mz_t}\end{bmatrix}=\begin{bmatrix}g(\eta_{ha}) & g(\eta_{hs}) & g(\eta_{vs})\\ & g(\eta_{ha}) & g(\eta_{vs})\\ sym. & & g(\eta_{va})\end{bmatrix}, \quad (7)$$

where $g(\eta_k)=1-\exp[-(\bar{a}I_1+\sqrt{J_2})^m/\eta_k^m]$ is the damage function, I_1 and J_2 are the first stress invariant and second partial stress invariant respectively, $\bar{a}$ is the constant in Drucker-Prager (DP) strength criterion; η_k is strength parameter in isotropic plane as η_{ha} or η_{hs}, in transverse direction as η_{va} or η_{vs} respectively; η_{ha} and η_{va} adopt the uniaxial compressive strength as the medium is compressive ($0\leqslant\sigma_i$, $i=1,2,3$) in principle direction, and vice versa, the uniaxial tensile strength would be adapted; η_{hs} and η_{vs} are the shear strength in isotropic plane and transverse direction respectively, which adopt the 0.8–1.0 times the tensile strength [37]. All these aforementioned strength parameters can be tested by traditional rock mechanical experiments.

The damage considering various factors, e.g. stress, chemical and temperature, could form a comprehensive damage variable. Using the hydration damage tensor eq. (6) and stress damage tensor eq. (7), the comprehensive damage tensor could be obtained as:

$$\boldsymbol{D}_t=1-(1-\boldsymbol{D}_c).\times(1-\boldsymbol{D}_m),\qquad(8)$$

where $1-\boldsymbol{D}_c$ represents the subtraction between scalar 1 and each parameter in tensor $\boldsymbol{D}_c$ to form a new tensor with the same number of rows and columns as $\boldsymbol{D}_c$, which rule goes for $\boldsymbol{D}_m$ and $\boldsymbol{D}_t$ in the same way; the notations ".×" represents the product of each corresponding parameter in two matrixes, so the coefficients in matrix $\boldsymbol{D}_t$ are operated by the corresponding coefficients in matrixes $\boldsymbol{D}_c$ and $\boldsymbol{D}_m$ with comprehensive consideration the current hydration and stress state.

5.2 Stress and permeability with damage

In TCS, the solutions of effective stress $\boldsymbol{\sigma}_t^{\mathrm{e}}$ and permeability $\boldsymbol{\kappa}_t$ have been computed by FEM in Section 4. Considering the effect of damage, the effective stress should be reduced by the damage tensor according to the strain equivalence principle [38]; the permeability of rock will enhance gradually due to the macroscopic damage generation and expansion, basing on relationship between permeability and strain [17,39], a reliable technology of effective stress and permeability damage evolution is proposed to reflect the damage characteristic as:

$$\tilde{\boldsymbol{\sigma}}_t=\boldsymbol{\sigma}_t^{\mathrm{e}}./(1-\boldsymbol{D}_t),\qquad(9a)$$

$$\tilde{\boldsymbol{\kappa}}_t=\boldsymbol{\kappa}_t.\times\exp(\gamma\boldsymbol{D}_t)(\varphi/\varphi_0)^3,\qquad(9b)$$

where the notations "./" represents the division of each corresponding parameter in two matrixes; $\boldsymbol{\sigma}_t^{\mathrm{e}}$ is effective stress in TCS; $\tilde{\boldsymbol{\sigma}}_t$ is stress with damage; $1-\boldsymbol{D}_t$ is the damage item to describe the enhancement characteristic of effective stress; φ_0 and φ are initial and current porosities respectively, γ is the permeability damage coefficient (here γ=0.5), and $\exp(\gamma\boldsymbol{D}_t)$ is the damage item to describe that the permeability is enhanced by damage. Through some numerical examples test including the results given below, eq. (9) describing the damage effect of stress and permeability reveals excellent effect.

6 Wellbore stability analysis based on weak plane strength criterion

The weak plane model is usually considered in most application cases, assuming a series of weak plane with a given orientation angle within the rock media as shown in Figure 6, a corresponding analytical method could be established. For wellbore stability analysis, the weak plane analytical method adopts Mohr-Coulomb criterion for compressive failure and tensile stress criterion for tensile failure in rock matrix and weak plane (or expressed as isotropic plane) respectively, the strength parameter values in rock matrix are higher than the corresponding values in weak plane. The weak plane strength criterion was introduced here to check the failure or not in laminated medium and using the transversely isotropic FE solutions.

The proposed method introduces the below weak plane strength criterion to check the strength for the transversely isotropic rock as:

tensile failure in weak plane

$$\tilde{\sigma}_{z_t}\leqslant 0,\qquad(10a)$$

compressive failure in weak plane

$$\tilde{\sigma}_1-\tilde{\sigma}_3\geqslant\frac{2(S_{\mathrm{w}}+\mu_{\mathrm{w}}\tilde{\sigma}_3)}{(1-\mu_{\mathrm{w}}\,\mathrm{ctg}\,\beta_t)\sin 2\beta_t},\qquad(10b)$$

tensile failure in rock matrix

$$\tilde{\sigma}_\theta\leqslant-\sigma_t,\qquad(10c)$$

compressive failure in rock matrix

$$\tilde{\sigma}_1-\tilde{\sigma}_3\geqslant 2(S_0+\mu_0\tilde{\sigma}_3)[(\mu_0^2+1)^{1/2}+\mu_0],\qquad(10d)$$

where components of stresses with damage in eq. (10) are all expressed in TCS, $\tilde{\sigma}_{z_t}$ is the normal stress of weak

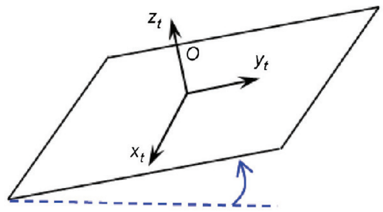

Figure 6 Weak plane and deviation angle β_t of laminated rock.

plane (or expressed as stress in transverse direction); $\tilde{\sigma}_1$ and $\tilde{\sigma}_3$ are the first and third principal stresses respectively; $\tilde{\sigma}_\theta$ is the tangential stress; S_0 and S_w are cohesions in rock matrix and weak plane respectively; μ_0 and μ_w are internal friction coefficients in rock matrix and weak plane respectively; σ_t is tensile strength in rock matrix. All these aforementioned strength parameters can be tested by traditional rock mechanical experiments. As shown in Figure 4, the stress results of the middle section in 3D FE model with well deviation angle and azimuth represent the stress state under the current pressure load of mud on borehole, so the weak plane criterion is used to check the stress as eq. (10). By increasing current pressure load (mud weight) and repeating application of the weak plane criterion for wellbore stability analysis, both of the collapse pressure (lower mud weight) and fracture pressure (upper mud weight) could be achieved as described in Section 3.

7 Numerical examples

The proposed analysis strategy has been coded into a Matlab program and partly used the transient FE solver of COMSOL Multiphysics basing on the FEA strategy. This section presents three interrelated numerical examples showing the performance of the procedure. Throughout, the program is run on a DELL OptiPlex 380 Intel(R) Core(TM) 2.93 GHz desktop computer. The first example is chosen to discuss the effectiveness for hydration effect of the proposed method with hydraulic-mechanical-chemical (HMC) coupling, by comparing the results of pore pressure and stress of rock surrounding wellbore with the poroelastic analytical method for transverse isotropic and isotropic cases. The second example analyzes change around the wellbore under the effect of the hydration effect, and the phenomenon of the physical property change over time. In last example, a practical shale engineering case, the collapse cycling time, time-dependent collapse and fracture pressure (safe mud weight) will be computed. In the three examples, the shape parameters m of Weibull distribution for heterogeneous material property and strength property are set as 5 and constant $\bar{a}$ in DP strength criterion is set as 0.29; when the FE procedure is implemented, the tetrahedral element is used and the adaptive error tolerance *tol* for FE mesh and error tolerance *Tol* for the upper bound and lower bound of mud weight are all set as 5% throughout.

7.1 Pore pressure and stress analysis of rock surrounding wellbore with HMC coupling

In this study, a special case for laminated rock with hydration effect is considered with the axis of material symmetry coinciding with the axis of the wellbore model as shown in the Figure 7, which analytical solutions exists [40]. The wellbore model was simulating a vertical wellbore to drill into organic-rich Woodford shale formation. The basic physical parameters of the model are listed in the Table 1, in which the parameter μ is the pore fluid viscosity coefficient.

Figure 8 presents pore pressure and effective stress distributions inside the model profile along the direction of the maximum horizontal stress S_H (A-B in Figure 7) at 15 min after drilling, as function of the normalized radial distance $r/(\bar{d}/2-d/2)$, $\bar{d}$ =300 mm is the diameter of the focus area, here r is the absolute radial distance form wellbore wall, normalized radial distance of zero and one correspond to the inner boundary and the outer boundary respectively. To further illustrate the effectiveness of the proposed method for this tight rock, results from the poroelastic analytical method for transversely isotropic and isotropic (E_h=E_v=4.2 Gpa, ν_h=ν_v=0.3) analyses are included. In order to be more effective for comparison with the poroelastic analytical results, the damage analysis and heterogeneity simulation of the proposed method are not considered in this example, in other words, just with HMC coupling and homogeneous media. It should be noted that the poroelastic analytical method using the generalized plane strain model for transversely isotropic case is just suitable for the the axis of material symmetry coinciding with the axis of the wellbore model, however the proposed numerical method can

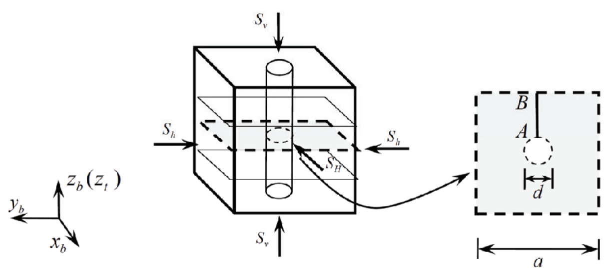

Figure 7 Wellbore model with axis coinciding with axis of material symmetry.

Table 1 Physical parameters for example 1

Parameter	Value	Parameter	Value
h (m)	2000	k_h (nD)	50
d (mm)	200	k_v (nD)	50
S_v (g/cm^3)	2.5	φ_0	0.15%
S_h (g/cm^3)	2.0	μ (Pa s)	1.0*E*-3
S_H (g/cm^3)	2.2	$w_{d/2}$	0.09
p (MPa)	19.6	w_∞	0.03
P (MPa)	21.4	c_h	0.0434
E_h (GPa)	7.4	c_v	0.0434
E_v (GPa)	4.2	$c_{\varepsilon 1}$	0.078
ν_h	0.13	$c_{\varepsilon 2}$	11.08
ν_v	0.30	c_e	11
α_h	0.85	c_V	1.3
α_v	0.88		

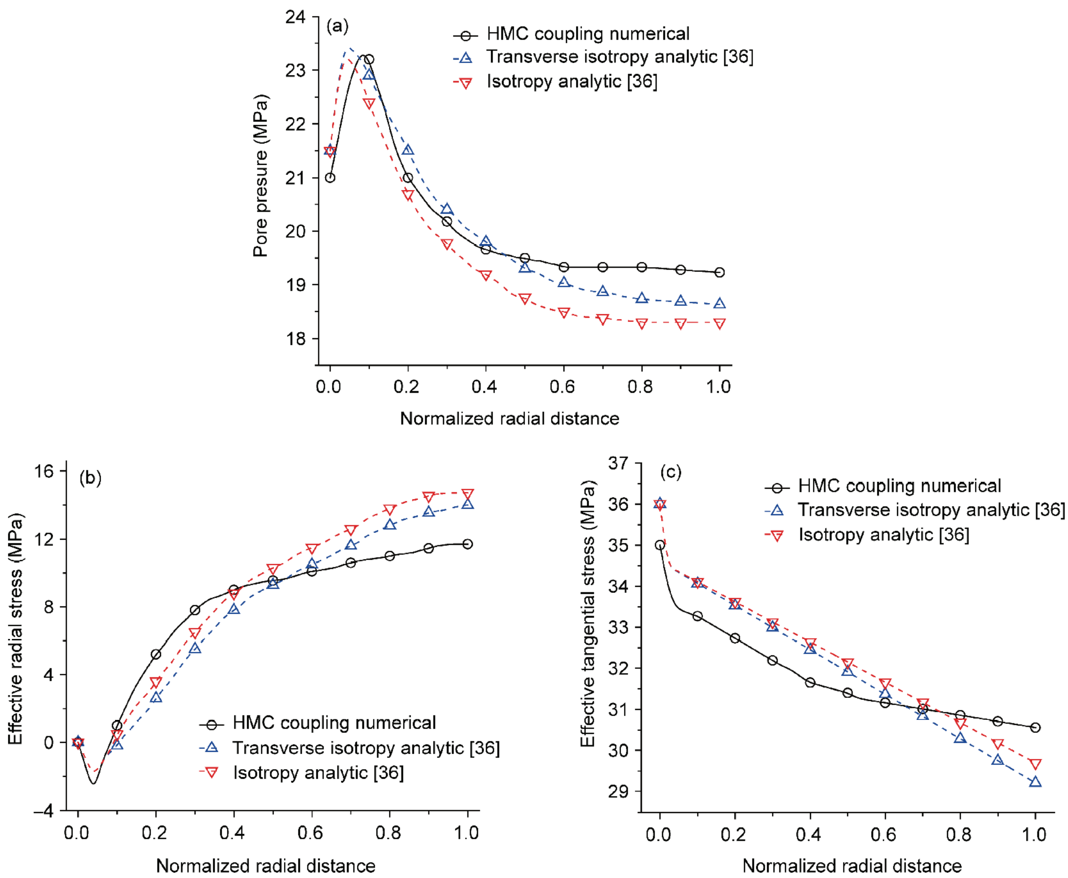

Figure 8 (Color online) Results comparison at time $\bar{t}$=15 min of proposed method and poroelastic analytical method. (a) Pore pressure results; (b) effective radial stress results; (c) effective tangential stress results.

handle the other inclined wellbore cases serving as a general method.

Figure 8(a) shows that the pore pressure results computed by the proposed method is consistent with the results of the poroelastic analytical method, the maximum pore pressure 23.5 MPa appear at normal radial distance 0.05 by the hydration effect of the mud activity and the minimum pore pressure blew the initial value 19.6 MPa appear at normal radial distance 0.5 as the result of the maximum horizontal stress. Figure 8(b) and (c) also shows the consistence of the effective radial and tangential stresses results of the proposed method with poroelastic analytical results. The radial stress results at normal radial distance about 0.04–0.05 achieve the minimum value, and the tangential stresses results decrease rapidly. Both of the effective radial and tangential stresses results at normal radial distance about 0.5 varies smoothly, which are slightly different from the analytic solutions.

7.2 Petrophysical heterogeneity and chemically active effect analysis

The effectiveness of the heterogeneous modeling and hydration analysis technologies will be revealed as below utilizing the FE model and the numerical computation in this paper. The geometric model is shown as Figure 5, the input parameters are provided by actual experiments of Longmaxi formation shale in Sichuan province in China as shown in Table 2 [41], $c_{\eta c}$ and $c_{\eta\varphi}$ are hydration constants for cohesion and internal friction coefficient respectively, other hydration parameters are the same as Section 7.1. The heterogeneous model is established using the Weibull distribution

Table 2 Physical parameters for example 2

Parameter	Value	Parameter	Value
h (m)	2500	S_0 (MPa)	9.2
d (mm)	215.9	S_w (MPa)	8.56
S_v (g/cm^3)	2.49	μ_0	0.716
S_h (g/cm^3)	2.26	μ_w	0.41
S_H (g/cm^3)	2.84	α_h	0.8
α_s (°)	N30°E	α_v	0.7
γ_t (°)	0°	k_h (nD)	500
E_h (GPa)	24.91	k_v (nD)	200
E_v (GPa)	14.093	φ_0	3.7%
G_v (GPa)	14.81	σ_t (MPa)	7
ν_h	0.26	$c_{\eta c}$	58.8
ν_v	0.3	$c_{\eta\varphi}$	2.8

with m=5 for initial parameters assignment, i.e. Young's modulus, shear modulus and permeability. For example, the probability density function of Weibull distribution for Young's modulus E_h with scale parameter n=24.9 GPa is shown in Figure 9(a). The 3D and the middle slice section of the wellbore model distributed as Figure 9(b) and (c), and it can be seen that the range of the values is about 27–29 GPa, which heterogeneous distribution has good consistency in the whole region. The revolution of some significantly time-dependent results, as moisture content, damage variable, elastic modulus and hydration strain of time $\overline{t}$ =10, 50 and 100 d, are shown and illustrated in Table 3. The moisture content (e.g. w_1) around the wellbore uniformly increases as the result of the same value as permeability setting in the isotropic plane. At time t=100 d, the moisture content extension outward is obvious and the radial distance of hydration almost reach 0.5 m, the damage (e.g. $\boldsymbol{D}_{11}$) at this time become serious, which would cause the phenomenon of diameter expansion and wellbore failure, so the exposed borehole is protected by casing in the actual petroleum drilling engineering. The Young's modulus (e.g. $\boldsymbol{e}_{11}$) is decreasing gradually with the moisture content increasing, which reveal the changing value is homogeneous and striped expansion as the result of the initial heterogeneity of rock. The maximum expansion stain (e.g. $\Delta\boldsymbol{\varepsilon}_{11}$) reach almost 0.06 to influence the stress distribution at the wellbore, which is difficult to be analyzed without considering hydration.

7.3 Time-dependent collapse and fracture pressure computation

This example will discuss the collapse cycling time, the collapse pressure (lower critical mud weight) and fracture pressure (upper critical mud weight) computed by the proposed method. The deviation angle of the isotropic plane is β_t=0° to reveal its influence on wellbore stability, and the other physical parameters and hydration parameters are the same as Section 7.2 listed in Table 2.

The collapse pressure results of different deviation angle β_b=0°, 30°, 60°, 90° at wellbore azimuth α_b=30° (the direction of the minimum *in-situ* stress S_h) are shown in Figure 10. It can be saw that the collapse pressure increase with β_b becoming bigger as the result of S_h. With the time increasing, the the collapse pressure results become bigger form smooth value until time reaching about 10 d, which is called the collapse cycling time. In the actual petroleum engineering, drilling fluid density need to increase as the time increasing for water-sensitive rock formation, the collapse cycling time need reliably predict to keep real-time wellbore stability.

Figure 11 shows the collapse pressure (lower critical mud weight) and fracture pressure (upper critical mud weight) at time 50 d computed by the proposed method, which polar plots have the symmetry at α_b=30°, 210° and α_b=120°, 300° (North direction as α_b=0°) with respective to the direction of the *in-situ* stresses due to the deviation an-

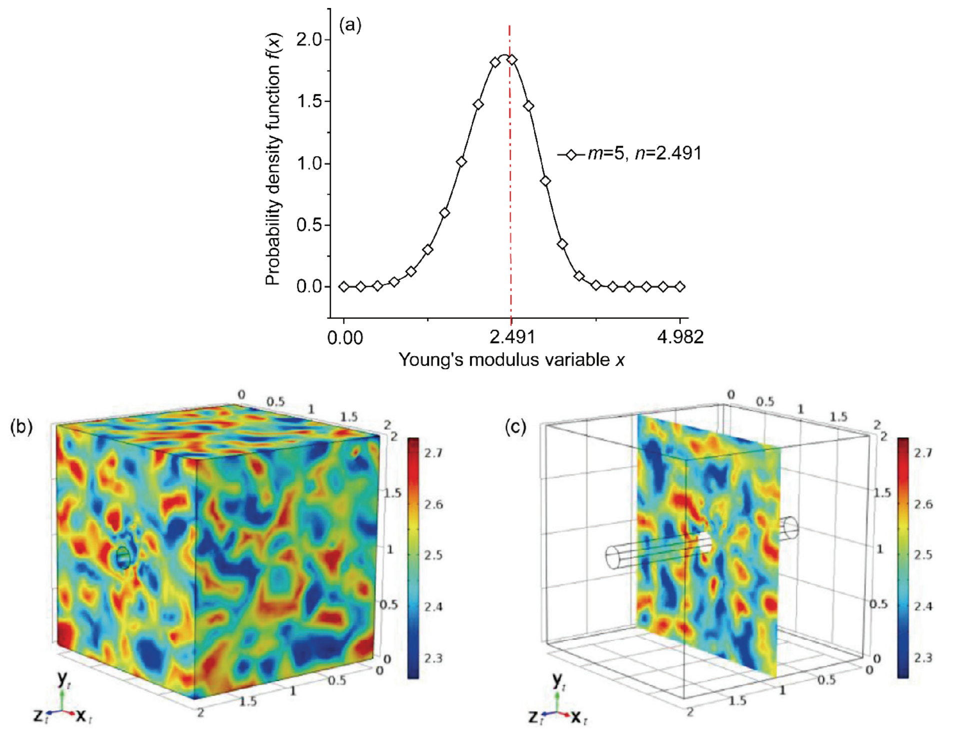

Figure 9 (Color online) Heterogeneous distribution of initial Yong's module E_h/10 GPa. (a) Probability density function of Weibull distribution; (b) 3D model; (c) 2D slice model.

Table 3 The revolution of time-dependent results, as moisture content, damage variable, elastic modulus and hydration strain

Time $\bar{t}$ (d)	Moisture content w_1	Damage variable $\boldsymbol{D}_{11}$	Young's modulus $\boldsymbol{e}_{11}$ (×10 GPa)	Hydration strain $\Delta\varepsilon_{11}$ (×10^{-2})
10	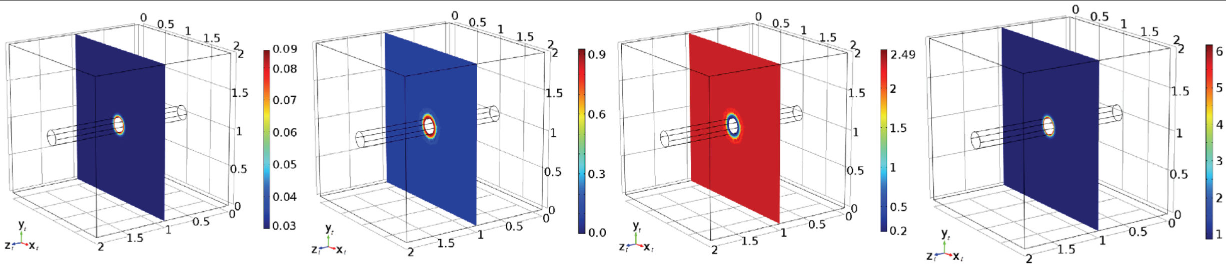			
50	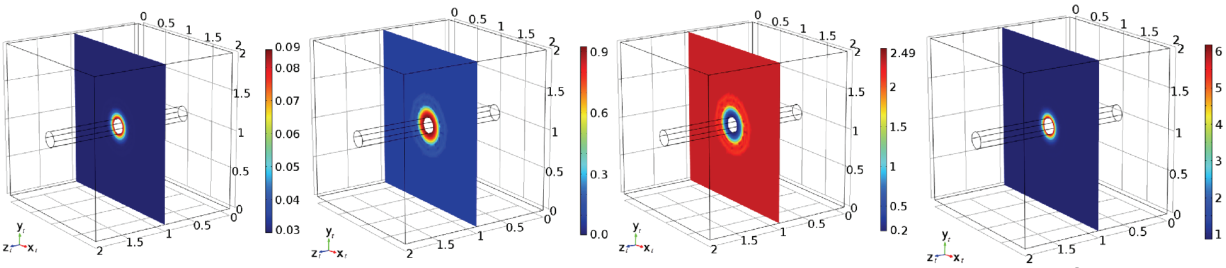			
100	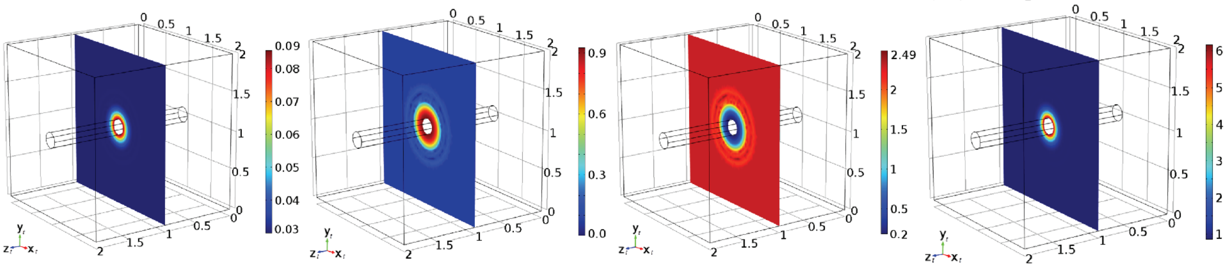			

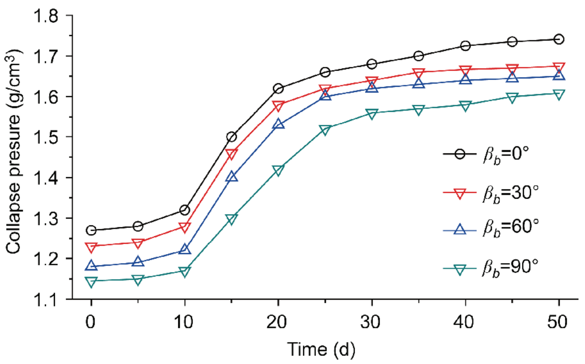

Figure 10 (Color online) Collapse pressure (lower critical mud weight) results computed by the proposed method at well azimuth α_b=30° and different deviation angles of β_b=0°, 30°, 60°, 90°.

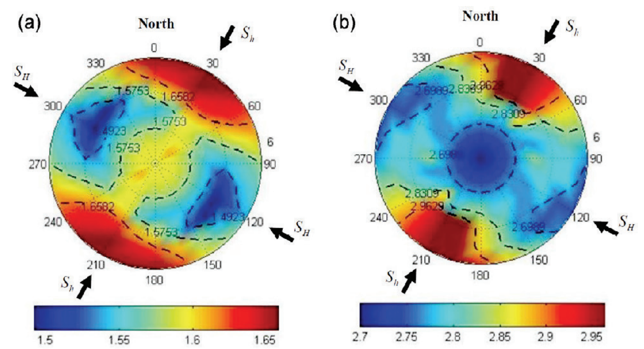

Figure 11 (Color online) Polar plots of (a) collapse pressure (lower critical mud weight) (g/cm^3) and (b) fracture pressure (upper critical mud weight) (g/cm^3) at time $\bar{t}$ =50 d computed by the proposed method.

gle of the isotropic plane setting as β_t=0°. It can be saw that both of the collapse and fracture pressure results are bigger in the direction of minimum *in-situ* stress as α_b=30°, 210° than the corresponding values in the direction of maxim *in-situ* stress as α_b=120°, 300°. In Figure 11(a), the collapse pressure become bigger with the deviation angles increasing in the direction of minimum *in-situ* stress as α_b=30°, 210°, on the other hand, the minimum collapse pressure appears almost at deviation angles β_b=60° in the direction of maxim in-situ stress as α_b=120°, 300°. In Figure 11(b), the fracture pressure become bigger with the deviation angles increasing in the direction of minimum *in-situ* stress as α_b=30°, 210°, on the other hand, the collapse pressure become smaller with the deviation angles increasing in the direction of maxim *in-situ* stress as α_b=120°, 300°. Comprehensive considering of the above analysis results, the drilling fluid density at each wellbore deviation angle and azimuth of inclined wellbore needs to be greater than the values in Figure 11(a) and be smaller than the values in Figure 11(b) for optimizing the drilling direction.

8 Conclusion

A new FEA technology with HMCD coupling for inclined wellbore stability analysis of transversely isotropic rock have been presented, which successfully has yielded a reliable FE procedure that obtains the results surrounding wellbore considering the chemical activity of the drilling fluid by phenomenological hydration behavior, furthermore the collapse cycling time was analyzed and the safe mud weight computation for collapse and fracture pressure were computed. For water-sensitive and laminated rock, comprehensive utilization of the classic Biot constitutive relation, damage tensor and weak plane strength criterion has described the anisotropic wellbore failure behavior for being consistent with the property of rock. One of the key techniques incorporated into this procedure is the technology transfer of HMD coupling to HMCD coupling by introducing the hydration effect. Results for typical numerical examples have shown that the present HMCD coupling analysis could obtain significantly different results from the case not considering the chemical activity of the drilling fluid and possesses the potential for further extension to practical engineering application. Using the FEA technology of the proposed procedure, anisotropic damage evolution and hydraulic fracturing for rock with multi-fields coupling have made some progresses, which will be reported in future publications.

This work was supported by the National Natural Science Foundation of China (Grant Nos. 11372157, 11302115 & 51608301), the Doctoral Fund of Ministry of Education of China (Grant No. 20120002110075), the Foundation for the Author of National Excellent Doctoral Dissertation of China (Grant No. 201326) and the China Postdoctoral Science Foundation (Grant No. 2015M571030).

Supporting Information

The supporting information is available online at tech.scichina.com and www.springerlink.com. The supporting materials are published as submitted, without typesetting or editing. The responsibility for scientific accuracy and content remains entirely with the authors.

1 Zhuang Z, Liu Z L, Wang Y L. Fundamental theory and key mechanical problems of shale oil gas effective extraction (in Chinese). Chin Q Mech, 2015, 33: 8–17

2 Lo T, Coyner K B, Toksöz M N. Experimental determination of elastic anisotropy of Berea sandstone, Chicopee shale, and Chelmsford granite. Geophys, 1986, 51: 164–171

3 Abousleiman Y N, Hoang S K, Tran M H. Mechanical characterization of small shale samples subjected to fluid exposure using the inclined direct shear testing device. Int J Rock Mech Min Sci, 2010, 47: 355–367

4 Yang H L, Shen R C, Fu L. Composition and mechanical properties of gas shale (in Chinese). Pet Drill Tech, 2013, 41: 31–35

5 Nguyen V X, Abousleiman Y N, Hoang S. Analyses of wellbore instability in drilling through chemically active fractured-rock formations. SPE J, 2009, 14: 283–301

6 Bažant Z P, Salviato M, Chau V T, et al. Why fracking works. J Appl Mech, 2014, 81: 1–10

7 Abousleiman Y N, Nguyen V X. PoroMechanics response of inclined wellbore geometry in fractured porous media. J Eng Mech, 2005, 131: 1170–1183

8 Nguyen V X, Abousleiman Y N. Naturally fractured reservoir three-dimensional analytical modeling: theory and case study. In: SPE Annual Technical Conference and Exhibition. Society of Petroleum Engineers, 2009

9 Chen S L, Abousleiman Y N. Stress analysis of borehole subjected to fluid injection in transversely isotropic poroelastic medium. Mech Res Commun, 2016, 73: 63–75

10 Hoang S, Abousleiman Y N, Ewy R T. Openhole stability and solids production simulation in emerging reservoir shale using transversely isotropic thick wall cylinders. In: SPE Annual Technical Conference and Exhibition. Society of Petroleum Engineers, 2009

11 Lu Y H, Chen M, Jin Y, et al. A mechanical model of borehole stability for weak plane formation under porous floe. Pet Sci Tech, 2012, 30: 1629–1638

12 Xiao Y, Liu H, Desai C S, et al. Effect of intermediate principal stress ratio on particle breakage of rockfill material. J Geotech Geoenviron Eng, 2016, 142: 06015017

13 Zhao Y P, Chen J, Yuan Q, et al. Microcrack connectivity in rocks: a real-space renormalization group approach for 3D anisotropic bond percolation. J Stat Mech: Theory Exp, 2016, 2016: 013205

14 Zhuang Z, Cheng B B. A novel enriched CB shell element method for simulating arbitrary crack growth in pipes. Sci China Phys Mech Astron, 2011, 54: 1520–1531

15 Zeng Q L, Liu Z L, Xu D D, et al. Modeling stationary and moving cracks in shells by X-FEM with CB shell elements. Sci China Tech Sci, 2014, 57: 1276–1284

16 Krajcinovic D, Lemaitre J. Continuum Damage Mechanics Theory and Applications. New York: Springer-Verlag, 1987

17 Zhu W C, Bruhns O T. Simulating excavation damaged zone around a circular opening under hydromechanical conditions. Inter J Rock Mech Min Sci, 2008, 45: 815–830

18 Lu Y L, Elsworth D, Wang L G. Microcrack-based coupled damage and flow modeling of fracturing evolution in permeable brittle rocks. Comput Geotech, 2013, 49: 226–244

19 Wang Y L, Liu Z L, Lin S C, et al. Finite element analysis of seepage in rock based on continuum damage evolution (in Chinese). Eng Mech, 2016, 33: 29–37

20 Wang Y L, Liu Z L, Yang H L, et al. FE analysis of rock with hydraulic-mechanical coupling based on continuum damage evolution. Math Probl Eng, 2016, doi: 10.1155/2016/8534965

21 Wang Y L, Liu Z L, Yang H L, et al. Finite element analysis for wellbore stability of transversely isotropic rock with hydraulic-mechanical-damage coupling. Sci China Tech Sci, 2017, 60: 133–145

22 Wang Y L, Zhuang Z, Liu Z L, et al. Finite element analysis of transversely isotropic rock with mechanical-chemical-damage coupling. Eng Mech, 2016, doi: 10.6052/j.issn.1000-4750.2016.04.0287

23 Mortara G. A yield criterion for isotropic and cross-anisotropic cohesive-frictional materials. Int J Numer Anal Met, 2010, 34: 953–977

24 Xiao Y, Liu H L, Yang G. Formulation of cross-anisotropic failure criterion for granular material. Int J Geomech, 2012, 12: 182–188

25 Hill R. The Mathematical Theory of Plasticity. Oxford: Oxford University Press, 1950

26 Pariseau W G. Plasticity theory for anisotropic rocks and soils. In: Proceedings of the 10th U.S. Symposium on Rock Mechanics. American Rock Mechanics Association, 1968. 267–295

27 Lee H, Ong S H, Azeemuddin M, et al. A wellbore stability model for formations with anisotropic rock strengths. J Pet Sci Eng, 2012, 96: 109–119

28 Lee H, Chang C, Ong S H, et al. Effect of anisotropic borehole wall failures when estimating *in situ* stresses: A case study in the Nankai accretionary wedge. Mar Pet Geol, 2013, 48: 411–422

29 Biot M A. General theory of three-dimensional consolidation. J Appl Phys, 1941, 12: 155–164
30 Biot M A. Theory of stress-strain relations in anisotropic viscoelasticity and relaxation phenomena. J Appl Phys, 1954, 25: 1385–1391
31 Detourmay E, Cheng A H D. Fundamentals of Poroelasticity. Oxford: Pergamon, 1993
32 Cheng A H D. Material coefficients of anisotropic poroelasticity. Inter J Rock Mech Min Sci, 1997, 34: 199–205
33 Dokhani V, Yu M, Takach N E, et al. The role of moisture adsorption in wellbore stability of shale formations: Mechanism and modeling. J Nat Gas Sci Eng, 2015, 27: 168–177
34 Huang R Z, Chen M, Deng J G, et al. Study on shale stability of wellbore by mechanics coupling with chemistry method (in Chinese). Drill Fluid Compl Fluid, 1995, 12: 15–21
35 COMSOL Multiphysics User's Guide. Version 5.0. Stockholm: COMSOL Inc., 2014
36 Jean L. Coupled elasto-plasticity and damage constitutive equations. Comput Methods Appl Mech Eng, 1985, 51: 31–49
37 Jaeger J C, Cook N G W. Fundamentals of Rock Mechanics. Houston: Blackwell Publishing, 1983
38 Krajcinovic D. Damage mechanics: Accomplishments, trends and needs. Inter J Solids Struct, 2000, 37: 267–277
39 Zhu W C, Bruhns O T. Simulating excavation damaged zone around a circular opening under hydromechanical conditions. Inter J Rock Mech Min Sci, 2008, 45: 815–830
40 Tran M H, Abousleiman Y N. Anisotropic porochemoelectroelastic solution for an inclined wellbore drilled in shale. J Appl Mech, 2013, 80: 020912
41 Yang H L, Chen C W, Wang J H, et al. Technical report of experimental study of shale drilling (in Chinese). Beijing: Drilling Research Institute, China National Petroleum Corporation, 2013